Journal of Theoretical and Applied Information Technology
15th May 2024. Vol.102. No 9

ISSN: 1992-8645 www.jatit.org E-ISSN: 1817-3195

EMBEDDED PATTERN ANALYSIS OF PLANAR PHASED ARRAY ANTENNA FOR X BAND COMMUNICATION SYSTEMS

KALAIARASI. D[1], M.R.EBENEZAR JEBARANI[2]

[1] ECE, Sathyabama Institute of Science and Technology, Chennai, Tamilnadu, India

[2] ECE, Sathyabama Institute of Science and Technology, Chennai, Tamilnadu, India

[1]kalai05art@gmail.com, [2]rjebamalgam@gmail.com

ABSTRACT

This study utilises the embedded element pattern to evaluate the Phased Array Antenna (PAA) in the context of the X-band communication system. All of them are linked to a finite array reference impedance. The central element of the embedded pattern is determined by a single element that is embedded within the finite array. The preparation of a Phased Array Antenna involves the use of a large number of radiating components that are connected to a phase shifter. This phase shifter is responsible for adjusting the phase of the radiating elements and producing a beam in the desired direction. PAA offers several advantages over a single radiating element, including increased power density, efficiency, directivity, and gain. This study examines the design and analysis of a rectangular phased array antenna commonly employed by military forces for satellite communications in the X-band frequency range.

Keywords - *Dipole Antenna, Directivity, Rectangular planar, Phased Array Antenna, Satellite Communication, X-band*

1. INTRODUCTION

Antenna arrays play a crucial role in wireless communication systems [1-11]. The present study explores the operational characteristics and benefits of Phased Array Antennas (PAAs), a technology that is extensively employed in many domains such as space exploration, defence, and radar applications. An effective antenna design is an essential requirement for enhancing the overall performance of the system. One illustrative instance pertains to a satellite communication system that employs a high-performance antenna in order to enhance the quality of transmission. The utilisation of Phased Array Antenna (PAA) is prevalent in various wireless communication systems, including but not limited to space research, defence, and radar applications. One primary rationale for employing PAA is its ability to attain a higher level of directivity in comparison to a single-element antenna [12-19]. The radiation pattern of an array antenna is influenced by various factors, including the individual radiating elements, radiation pattern, separation distance between antenna elements, amplitude and phase shift of antenna elements, and array arrangement. The electrically steerable mechanism in the PAA system enables the maximisation of gain or efficiency. This mechanism allows for the control of the signal in all directions by manipulating the steering angle, without the need for mechanical antenna movement [20-25]. The PAA is regarded for its ability to eliminate mechanical faults, immediately position beams, and track across vast distances. In the PAA, every radiating element is connected to a phase shifter. In order to generate a beam in the desired direction, phase shifters are employed to manipulate the phase shift of individual radiating elements. Each phase shift driver incorporates a bias current and voltage to effectively guide the beam towards the desired direction. The emission patterns of the antenna elements exhibit positive inhibition in the desired direction and significant inhibition in the undesired direction throughout the process of beamforming. The antenna beam of PAA may be electronically manipulated, enabling it to simultaneously track many targets in space. The utilisation of a phased array mitigates the impact of multipath fading on the communication link, resulting in an enhancement in the channel capacity. One

additional advantage of Passive Authentication (PAA) is its ability to enhance the security of communication connections by introducing null values in the undesirable signal direction. The PAA is comprised of a beamforming array of radiating elements, in addition to the power distribution of the RF feed network. PAA involves the generation of many radiating elements from a single source. By manipulating the array excitation in the PAA, it is possible to generate null radiation patterns. The PAA directive pattern is formed by the vector addition of separate radiating elements. The radiating element's performance is compromised when it collides with itself in the desired direction and in the surrounding space.

A phased array antenna refers to a design that consists of numerous antennas. The arrangement of antenna elements in linear or planar arrays enhances the antenna's directivity and gain. Multiple antenna elements collaborate to generate radiation characteristics that surpass the capabilities of a solitary antenna. The radiation pattern can be electrically modified by adjusting the phase and amplitude, so aligning it with the desired coverage region. Additionally, they possess the capability to conduct beam scanning inside an antenna system, enhance directivity, and execute a diverse range of jobs that pose challenges when relying solely on a single element. The items inside a feed network arrangement have the potential to get nourishment from either a single line or multiple lines. A array can be classified into three distinct kinds. Linear arrays, planner arrays, and conformal arrays are the three distinct forms of arrays. Phased array antennas are employed in communications and radar to provide far-field beam modelling and directing for unique, dynamic operational conditions. Current adaptive radar systems that employ advanced space-time adaptive signal processing and active phased arrays demonstrate a notable level of effectiveness. The primary benefit of PAA is the ability to electronically manipulate the antenna elements in a precise direction. Therefore, the PAA has the capability to communicate with several targets concurrently. This is especially advantageous for minimising the dissipation of radiated energy in the unwanted direction, as observed in omnidirectional antennas. Furthermore, the implementation of PAA's primary beam steering technique results in a reduction of multipath, pathloss, and fading effects on the communication connection, thus leading to an increase in channel capacity [26-30]. PAA also offers the capability to enhance signal security by impeding undesirable signals, such as those aimed at unauthorised access to a private network or jamming the communication system. The PAA system's sensitivity to the beamforming network needs a costly and complex calibration and manufacturing method due to the high cost of manufacture. This limitation restricts the remarkable potential of the PAA [26-30]. Solid-state active photoacoustic amplifiers (PAAs) gained popularity over time owing to their advantageous characteristics such as low weight, power dissipation, high output power, and reliability. However, the high production costs associated with these PAAs have constrained their utilisation mostly to radar applications within the military sector. The primary limitations of the active PAA are its intricate circuitry and exorbitant production expenses, which have restricted its implementation in the public sector. Recent improvements in PAA technology have made it possible to create a low-cost, high-performance integrated phased array antenna.

Although this research thoroughly examines the benefits and practical uses of PAAs, it refrains from delving into intricate design methodologies or precise implementation techniques. Furthermore, a comprehensive analysis of the historical progression of antenna technologies and a thorough comparison with alternative antenna configurations are absent from the text.

2. RELATED WORK

The design of the PAA mainly depends on the following parameters:

i. Overall configuration based on geometrical shapes such as circular, rectangular and elliptical, etc.,
ii. Individual radiating element amplitude and phase, spacing among antenna elements,
iii. The radiation pattern of individual antenna elements,
iv. The array configuration's total number of elements,
v. Side Lobe Level, Gain or Directivity, and Beamwidth

The significance of grating lobes in a beam former is elucidated in Paper [29]. Furthermore,

the various characteristics of the FPA antenna are thoroughly examined from the perspective of a designer for evaluation. This paper also emphasises the applications of limited scan PAA. The study thoroughly examines three distinct LSPAA topologies, incorporating MATLAB simulation outcomes. A Factor of Comparison (FOM) is also offered as a method for comparing them. The prototype of a low-profile millimeter-wave phased-array antenna for synthetic aperture radar (SAR) comprises several components, namely the antenna unit, feeding network, power network, and wave control network, as stated in reference [5]. The streamlined design of the phased array antenna is achieved by integrating the transceiver channel into the multi-function transceiver chip. The construction of the phased array antenna reduces its thickness to fulfil the requirements for thinness and modularity, with diameters of 130 mm, 80 mm, and 45 mm. A millimeter-wave phased-array antenna can satisfy the criteria for airborne synthetic aperture radar (SAR) with a scan range of 45 degrees, a transmission EIRP of 51dBm, and cross-polarization performance beyond 30dBc.The antenna array parameter "Array Factor" is graphed individually for each array in Paper [1]. A planar antenna array with dimensions N x N (where N ranges from 2 to 32) is created using MATLAB code. The "Array Factor" parameter is graphed individually for each array. An investigation was conducted to examine the impact of including antenna elements on the array factor. The directivity of the beam array factor of an antenna array is enhanced by increasing the number of antenna elements. The design of a rectangular patch Microstrip antenna is conducted through simulations, and its response is assessed by examining the design characteristics of phased array antennas. A 1x4 array is utilised to generate the radiation pattern, which is subsequently printed for the purpose of testing and analysis. The observed results align with the predictions made in the simulations. As a result, this architectural design has the capability to support arrays of any size. The performance of a Microstrip Line-fed Rectangular Microstrip Patch Antenna with dimensions of h-1.57mm, L-85mm, W-87mm, and a dielectric constant of 2.2 is examined at a frequency of 1.35GHz. The results indicate that this design is suitable for optimal performance. This study introduces a novel thinning array antenna that exhibits a visually appealing radiation pattern at a frequency of 28 GHz, specifically designed for 5G wireless applications [24]. The proposed thinned-array antenna, consisting of 34 elements, has exceptional performance in terms of suppressing side lobes. The 8 dBi broadside uniform array antenna exhibits a 3.1 dBi decrease in Maximum Side Lobes (MSL) in the E-plane and a 5.7 dBi decrease in the H-plane, despite the strength being just 1 dB lower. Compared to an 8-by-4 broadside uniform array antenna, the gain is 1.2 dBi higher and the MSL is 4.4 dBi lower, even if the H-plane MSL is 0.5 dBi higher. Reference [22] The device showcases a 1/8 phased array antenna designed for 5G applications, operating at a frequency of 28 GHz and featuring a higher HPBW. This study introduces a validated impedance matching technology. The proposed design has demonstrated exceptional impedance matching, ample peak gain, little side lobe level, satisfactory scan reporting, and a broad high-pass bandwidth (HPBW) in the elevation plane. The inclusion of air-hole holes results in a significant increase of more than 20 degrees in the HPBW as compared to the elevation plane. Due to its wide high-pass bandwidth (HPBW) in the elevation plane and satisfactory radiation qualities, the proposed array antenna has the potential to be a strong candidate for mm-wave 5G mobile device applications [21–24]. A letter [30] proposes an efficient pattern reconstruction method for phased array antenna radiation measurements in order to decrease measurement time and complexity. The calculation of patterns in the required beam directions is performed using the lowest norm least-square solution, which accounts for mutual coupling effects among the elements. The superiority of the beam arrangement refinement is demonstrated through comparisons between the reconstructed pattern and the desired or real pattern. The reconstructed pattern exhibits a strong resemblance to the required pattern due to its incorporation of co- and cross-polarization patterns at many scanning angles. Subsequent investigations will juxtapose the approach with the results obtained from the empirical array, encompassing not just mutual coupling but also additional factors.

Despite extensive research and development in PAA technology, there remains a gap in understanding the practical implications of these challenges and identifying effective solutions to address them. Current literature primarily focuses on theoretical aspects and performance

evaluations under ideal conditions, overlooking real-world constraints and limitations in PAA deployment.

The objective of this study is to comprehensively investigate the technical complexities, cost considerations, and performance optimization limitations associated with Phased Array Antennas in wireless communication systems. Through empirical analysis and case studies, the research aims to identify practical strategies for mitigating these challenges and enhancing the effectiveness of PAAs in diverse operational scenarios.

3. PLANAR PHASED ARRAY ANTENNA

The ideal antenna element is an isotropic one that radiates evenly in all directions. Although an isotropic radiation pattern is not desirable, a more directive pattern in the desired direction is necessary for practical applications. The ability to radiate energy in the desired direction is called directivity. The directivity is calculated as

$$D_{max} = \frac{4\pi}{\lambda} A \quad (1)$$

Where λ indicates the free-space wavelength and A denotes the physical area of the antenna. The directivity of the antenna can be increased by enlarging electrically the size of the antenna. Using an array antenna, which combines numerous antenna elements, the electrical size of the antenna can be enhanced. The directivity is related to antenna gain as follows

$$G = e_{rad} D \quad (2)$$

Where e_{rad} is called the radiation efficiency of the antenna. Because the antenna array has a larger gain than a single antenna element, it is employed to transmit the signal over longer distances. Hence, the antenna array is used in satellite communication and radar applications were transmitting the signal for a longer distance is required.

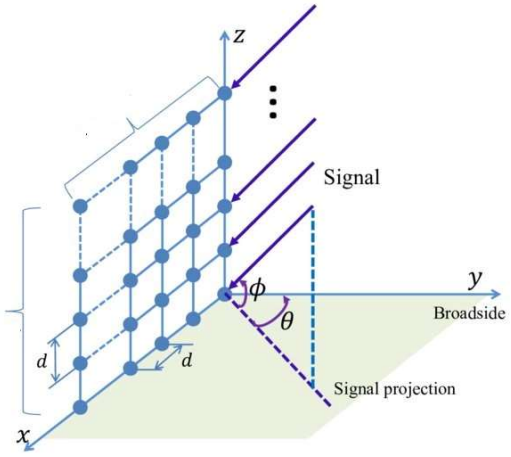

Fig. 1 Planar Phased Array Antenna

The Planer Phased Array Antenna (PPAA) contains equally spaced antenna elements that are stimulated in amplitude and phase. A rectangular two-dimensional linear array with equally spaced antenna elements is known as a planar array. The radiation field of a planar array, like that of a linear array, is the sum of the radiation from each radiating antenna element. The planar array radiation pattern is calculated using the azimuth and elevation angles. At the reference site, the radiation from PPAA is computed by multiplying the array factor by the field of a single antenna element. The array factor of an antenna array system is closely related to the radiation pattern. A matrix is multiplied by the array factor. The Equation 3, is used to calculate the total number of radiating elements in the PPAA.

$$\sum_{m=1}^{M} \sum_{n=1}^{N} l_{mn} \quad (3)$$

Where, M and N denotes the number of rows and columns in the planar array. The array factor for PPAA is expressed by the equation

$$AF = \sum_{m=1}^{M} \sum_{n=1}^{N} e\lambda^{\frac{j2\pi}{\lambda}[(d_x)_{mn} \sin(\theta) \sin(\varphi) + (d_y)_{mn} \sin(\theta) \sin(\varphi)]} \times l_{mn} \quad (4)$$

Where the distances in two dimensions in the planar array from a reference point are $(d_x)_{mn}$ and $(d_y)_{mn}$ respectively. On a linear surface, antenna arrays can be arranged in a row, in a grid on a flat surface, or a circular arrangement. Broadside and end-fire radiation patterns are two types of radiation patterns that can be seen in antenna arrays. Array antennas

can be classified into two classes based on how their main beam is meant to radiate: broadside and end-fire. The main beam of an end-fire array is directed along with the array, but the broadside array radiates perpendicular to the array's orientation, as shown in Figure 1. The direction of the beam can be adjusted without rotating the antenna platform if the array is phase steered. The antenna radiation pattern consists of the main lobe and side lodes. All the power radiated by the antenna is not concentrated on the main lode but some of the power will be leaked into the side lobes. This leaked power is called Side Lobe Level (SLL) and it can be expressed as

$$SLL = \max_{\theta,\varphi} AF(\theta,\varphi) \quad (5)$$

Due to the finite surface of the array, the side lodes are forming in the radiation pattern from less than -90° and more than 90°. The reduction of SLL can be obtained by using the tapering method by reducing the signal amplitudes towards the edges resulting in a wider main beam. The radiation field of antenna elements can be measured in two areas: near field and distant field. When determining the radiation pattern of an antenna, the far-field region is favoured. The spherical wave front from the antenna array is closely approximated with the ideal planar phase front of a plane wave. The far-field radiation pattern relationship can be represented using the equation below.

$$r \geq \frac{2D^2}{\lambda} \quad (6)$$

Where r denotes the antenna's radius, D the antenna's largest aperture area, and w the wavelength. The integral coupling formula derived from the far-field pattern is used to calculate the phased array antenna's near-field power densities. The comprehensive applicability of the integral coupling formula to a variety of microwave antennas is illustrated by the accessibility of the far-field radiation pattern. In terms of input data, precision, and processing time, the correctness of the formula is tested using the ideal circular aperture. The main beam variance is less than 0.7–1.2 dB, but the side lobe variation is 3–4 dB [28], and it takes only a few seconds to compute. For phased array antenna applications, a simple and low-cost 1 x 8 adaptive beam former with scalability in amplitude and phase has been designed. The frequency range in which the structure operates is 1.74 to 2.06 GHz, with a 0.8 dB average amplitude imbalance and an average phase deviation. At the central frequency, the RL might drop as low as 35 dB. The structure's radiation properties were examined by attaching an 8-element antenna array to the network's output; the measured main lobe was found to be extremely close to the theoretical one, while the SLLs were suppressed sufficiently [20]. The proposed modular design might simply be extended to a 1 X N beam former to achieve the desired results.

3.1 Computation of Far-Field in Planar Array Antenna

In this section, the far-field pattern is computed for the planar array. N rows M columns are considered in the planar array, and F is assumed to be the far-field in the direction of (θ, φ). The spacing between the antenna element in the x and y direction is assumed as d_x and d_y . The F is expressed in mathematically

$$F(u,v) = d_x d_y \sum_{m=1}^{M} \sum_{n=1}^{N} f_{mn}(u,v) A_{mn}\, e^{jk(md_x u + nd_y)} \quad (7)$$

where f_{mn} denotes a normalized embedded pattern of element (m,n), A_{mn} denotes complex excitation, k denotes the wavenumber $2\pi/\lambda$ and the direction cosines are given by $u = sin\theta cos\varphi$ and $v = sin\theta sin\varphi$. Considering that the aperture edge effects are neglected under large-array approximation, the pattern for normalized embedded elements can be represented as

$$F(u,v) = d_x d_y f(u.v) E(u,v) \quad (8)$$

$$E(u,v) = \sum_{m=1}^{M} \sum_{n=1}^{N} A_{mn}\, e^{jk(md_x u + nd_y)} \quad (9)$$

Where $E(u,v)$ denotes the array factor.

3.2 Embedded Element Pattern

The normalized embedded pattern for a large PAA can be written as

$$|f(\theta,\varphi)|^2 = cos\theta[1 - |\Gamma(\theta,\varphi)|^2] \quad (10)$$

Where Γ denotes the array's scan reflection coefficient in the computation of the far field.

3.3 Illumination Error Correction and Array Calibration

Antennas in a phased array can compensate for illumination flaws in the array. By adjusting the phase shifters of the array members appropriately, phase errors can be minimized. Amplitude mistakes can be minimized if the transmitting and receiving modules have independent amplitude control. The Digital Beam Former (DBF) has been proved to be a feasible controller for a Phased Array Antenna. The PAA measured findings revealed an increase in sidelobe level due to gain/phase shifts in linear amplifiers, mixers, and power amplifiers [19]. This can be corrected by calibrating each PAA channel while calculating the DBF channel's complex weight, taking into account the error generated by the RF components in the current distribution on the array's antennas. As a result, the PAA's digital control architecture allows for more design flexibility at each level, making it perfect for applications that require precise beam pattern control. Periodic array calibration gathers information on aperture-illumination errors in order to correct illumination errors. The precision of this error correction is determined by the degree of phase and amplitude quantization used by transmitting-module control devices and receiving-module control devices. When resolving amplitude issues, it is crucial to examine the nominal amplitude setting of the transmitting and receiving modules, as well as the adjustment range for the amplitudes.

4 SIMULATION RESULT AND ANALYSIS

For rectangular array architecture, we simulate the following change in variables:

1. Rectangular Array of N x M Dimensions
2. Element Spacing d_x and d_y
3. Current distribution: uniform or binomial
4. To emulate a pure Array Factor, use 0.5 dipoles or isotropic sources.
5. Beam direction φ_0 & θ_0 or phase distance α_x & α_y

Table 1. Summary of Array Configuration

Array type	Rectangular
Array element	Half-wave dipole
Polarization	Horizontal
No. of elements	11X11
Scanned angle	15o
Frequency	2.0 GHz
Vertical 3dB BW	12.7o
Side-lobe suppression	-20dB 1st side-lobe w.r.t main beam
Directivity	15.1 dBi

This simulation demonstrates how to create enormous discrete arrays with embedded element patterns. This approach is only applicable to extremely large arrays, as edge effects can be ignored. By driving the array's central element and terminating all other elements in a reference impedance, it is possible to determine the pattern of a single element embedded in a finite array. The embedded element, which is the pattern of the driven element, incorporates the coupling effect with neighboring components. Whether the array comprises an even or odd number of elements, the embedded element is typically selected from the array's central section or element (for large arrays, it does not matter). When an isolated element (a radiator put alone in space) is grouped in an array, the pattern of the isolated element (the radiator placed alone in space) alters due to reciprocal contact. As a result, pattern multiplication is no longer useful because it presupposes that everything has the same pattern. We can figure out how the total array radiation pattern will look by multiplying patterns. Replace the isolated element pattern with the one that arrives with each array element to achieve the better performance. As indicated in the introduction, this simulation demonstrates the use of the embedded element pattern when modelling large finite arrays. To accomplish this, we'll use the two arrays below: Compare the results to two array solutions based on the full-wave Method of Moments (MoM), one with isolated components and the other with embedded elements. The scanning performance of the array has been determined on both the broadside and off-broadside. Finally, we change the spacing of the arrays to see if scan blindness happens. Then, we compare the results to previous research works.

Journal of Theoretical and Applied Information Technology
15th May 2024. Vol.102. No 9

ISSN: 1992-8645 www.jatit.org E-ISSN: 1817-3195

The suggested 11 X 11 element planar phased array antenna at 2.0GHz was fully modelled and simulated using Matlab in this study. The software simulation is utilised to analyse the antenna's performance in relation to its shape, namely the coupling interaction between the array parts and the field networks. The absence of phase excitation results in the maximum radiation direction being at 0 degrees. The absence of a grating lobe is observed, and the level of the first side lobe (FSL) in relation to the main beam is measured to be 13dB lower than the main lobe. The distance from the main lobe is considerable, suggesting a minimal presence of undesired interference. However, it does not align with the intended alignment of 20dBi below the main lobe. The achieved beamwidth values for the -3dB simulation are 8.520 and 17.76dBi, respectively. The radiation pattern generated by the amplitude excitation effect exhibits a beamwidth of 23 degrees, with a magnitude of 3 decibels. Additionally, the side lobes are relatively large, rendering them unsuitable for the majority of applications. Elevated sidelobes have the potential to magnify interference and result in the reception of erroneous signals. Consequently, it is necessary to employ a taper in the amplitude of the element in order to reduce the beamwidth and level of side lobes [4, 5]. The observed radiation pattern has a beamwidth of 9.10 degrees, surpassing the value depicted in Figure 5. Additionally, there is a noticeable decrease in the presence of side lobes. Similarly, the directivity experiences a decrease from 17.76dBi to 17.19dBi. The FSL, on the other hand, is 19.8dBi lower than the main beam, which closely aligns with the design standard of 20dBi.

Model a dipole array with the Isolated Element Pattern. As mentioned in [4, the basic element of an 11 x 11 array begins to behave as though it were part of an infinite array. A ten-by-ten array of half-wavelength-spaced radiators would be required for such an aperture. We'll use an 11 x 11 dipole array, which is slightly larger than this limit. As our element, we'll deploy a dipole. Its length should be somewhat reduced, while its diameter should remain roughly the same. Compare the array patterns in Figures 2 and 3 in both the elevation and azimuth planes. The elevation and azimuth planes, commonly known as the E and H planes, are used to calculate each of the three arrays: isolated element pattern, embedded element pattern, and full-wave model. This is because the E plane is also known as azimuth = 0 degrees.

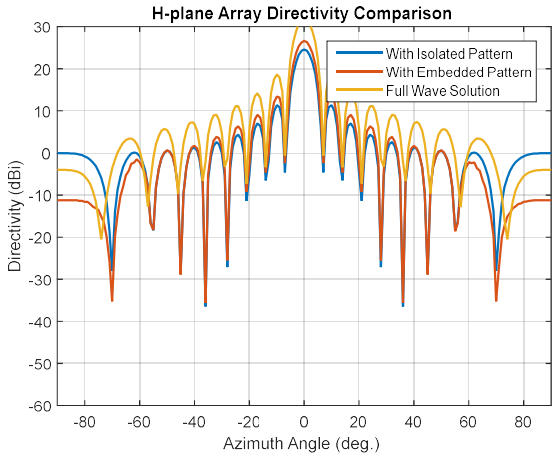

Fig. 2 Comparison of the Array Directivity of the H-plane

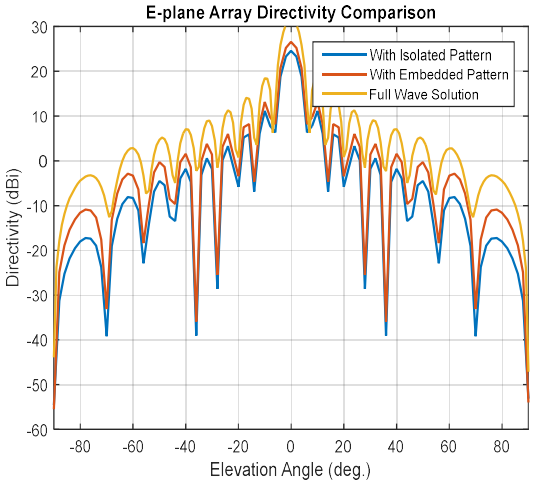

Fig. 3 Comparison of the Array Directivity of the E-plane

Consider the array's directivity is roughly 23 dBi. After taking into account the lack of a reflector,

$$D_{max} = \frac{4\pi}{\lambda mn} A \quad (11)$$

Where $A = d_x d_y$

This result is very near to the peak directivity estimate that was projected. Figures 4 and 5 show how to visualize and compare the three arrays by normalizing their directivity. In all

Journal of Theoretical and Applied Information Technology
15th May 2024. Vol.102. No 9

ISSN: 1992-8645 www.jatit.org E-ISSN: 1817-3195

three cases, the primary beam and early side lobes appear to be aligned, according to the pattern comparison. You can see how coupling has an increasing effect on the side lobe level as you go away from the main beam. According to the embedded element pattern strategy, the overall wave simulation model and the isolated element pattern technique will interact in some way.

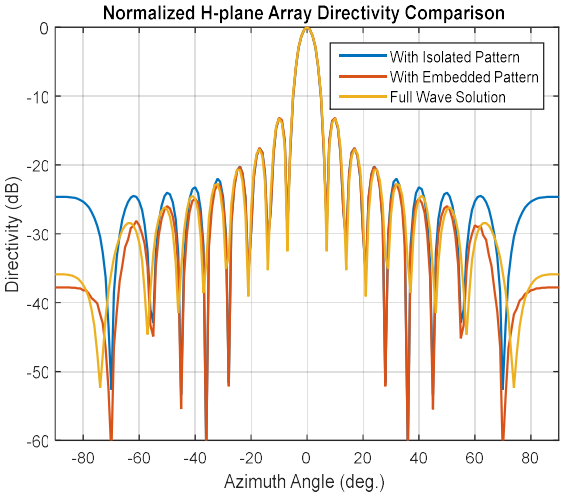

Fig. 4 Comparison of Array Directivity of Normalized H-plane

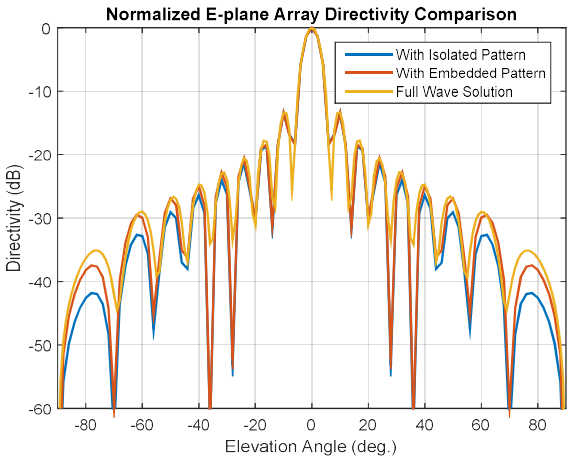

Fig. 5 Comparison of Array Directivity of Normalized E-plane

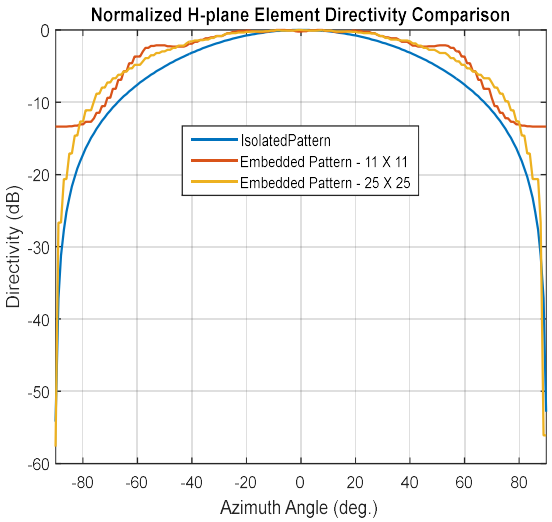

Fig. 6 Comparison of Element Directivity of Normalized H-plane with isolated pattern, and embedded pattern.

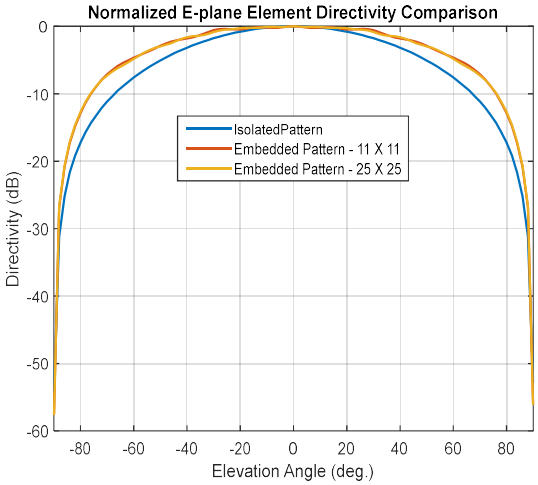

Fig. 7 Comparison of Element Directivity of Normalized E-plane with isolated pattern, and embedded pattern.

Compared to a 25 x 25 array, the behavior of the array pattern is intrinsically tied to the embedded element patterns in Figures 6 and 7. To examine how our 11 X 11 array influences the center element behavior, we increase the array size to a 25 X 25 array (12.5 X 12.5 aperture size). It's worth mentioning the

triangular mesh size for the whole wave Method of Moments (MoM) analysis.

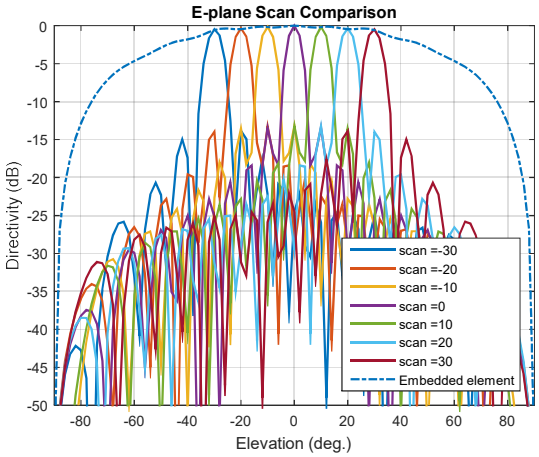

Fig. 8 Comparison of E-plane scan

Figure 8 depicts the effect of activating each element in the array with a different phase, guiding the beam in a certain direction with the amplitude taper on the radiation pattern. As the array is scanned, the beamwidth becomes wider. The complete pattern is displaced from the broadside pattern when the beam is scanned at an angle of 15o at the resonance frequency of 2.0GHz. Gating lobes are also visible. The element spacing (d) is lowered from 0.7 to 0.5 to eliminate the effect of the grating lobes. The settings for the amplitude and phase taper were tweaked significantly, resulting in variations in both directivity and 3dB beamwidth. 15.4dBi Directivity and 15.0o are the optimal values for the proposed antenna.

5 CONCLUSIONS

Simulations are employed in the construction of a planar phased array antenna and the subsequent evaluation of its response, drawing upon research conducted on the design features of phased array antennas. One method for studying large finite arrays is through the utilisation of embedded element pattern techniques. The impact of edge effects must be sufficiently negligible to evade detection. The isolated element pattern is replaced by an embedded element pattern that incorporates the mutual coupling effect. The observed results align with the predictions made in the simulations. Consequently, this architecture is capable of accommodating arrays of any size.

5.1 Future scope

Extending the study to three-dimensional phased array configurations offers opportunities for application in radar systems, satellite communications, and wireless networks. Integration with advanced beamforming algorithms could improve performance in dynamic environments, while exploring applications in next-generation communication systems such as 6G networks can address evolving connectivity needs. Furthermore, the development of compact and lightweight designs suitable for portable devices and UAVs presents an exciting area for exploration. These research directions aim to push the boundaries of planar phased array antenna technology, leading to enhanced communication systems and wireless technologies

REFERENCES

[1] P. s. v. Kumar, “N × N antenna array simulations using mat lab, International journal of innovative research in electrical, electronics, instrumentation and control engineering vol. 3, no.5, 2015.

[2] Y. Madhuri and B. Suresh, “Design aspects of Phased Array Antenna at L-Band,” International Journal of Engineering and Advanced Technology (IJEAT). no. 4, pp. 328–331, 2013.

[3] Chen, Tengbo, Zinan Ni, and Tao Zhang. "A calibration method of absolute time delay for phased array antenna." Journal of Physics: Conference Series. IOP Publishing ,Vol. 1087. No. 4, 2018.

[4] W. P. M. N. Keizer, “APAS : An Advanced Phased-Array Simulator,” IEEE Antennas and Propagation Magazine vol. 52, no. 2.2010

[5] Jihao, Li, Yang Zhenfeng, Li Yibing, Sun Xiaohang, Lv Ji, and Zhong Wei. "Research on low-profile millimeter wave phased array antenna for SAR." In 2019 6th Asia-Pacific Conference on Synthetic Aperture Radar (APSAR), IEEE,, pp. 1-4. 2019.

[6] Hilbertsson, Jenny, and Josefina Magnusson. "Simulation and evaluation of an active electrically scanned array (AESA) in Simulink." Master's thesis, 2009.

[7] G. Yang, S. Member, and Q. Chen, “Improving Wide-Angle Scanning Performance of Phased Array Antenna by Dielectric Sheet,” IEEE Access, vol. 7, pp. 71897–71906, 2019.

[8] Slovick, Brian A., Jeffrey A. Bean, and Glenn D. Boreman. "Angular resolution improvement of infrared phased-array antennas." IEEE Antennas and Wireless Propagation Letters vol.10,pp.119-122.
[9] Elhefnawy, Mohamed, and Azremi Abdullah Al-Hadi. "A novel design of slotted waveguide phased array antenna." Advanced Electromagnetics vol.8, no. 3 16-22, 2019.
[10] Alade, M. O., and E. P. Ogherowo. "Design and Analysis of 15.4 dBi, 8-Element Phased Array Dipole Antenna resonating at 2.0 GHz for Mobile Communication Applications." Science Journal of Physics 2015.
[11] Gashaw, Haylemaryam, Ayele Shumetie, Yonatan Tekle, and Swaminathan Ramamurthy. "Performance Analysis of Phased Array Antenna." International Journal of Advanced Research in Electronics and Communication Engineering (IJARECE), Vol.8.no.8, 2019.
[12] Kaur, Amandeep. "Electronically Steerable planer Phased Array Antenna." International Journal of Engineering Trends and Technologie vol.3, no. 6 708-709. 2012.
[13] Gu, Xiaoxiong, Duixian Liu, Christian Baks, Ola Tageman, Bodhisatwa Sadhu, Joakim Hallin, Leonard Rexberg, Pritish Parida, Young Kwark, and Alberto Valdes-Garcia. "Development, implementation, and characterization of a 64-element dual-polarized phased-array antenna module for 28-GHz high-speed data communications." IEEE Transactions on Microwave Theory and Techniques, vol. 67, no. 7,2975-2984.2019.
[14] Helander, Jakob, Kun Zhao, Zhinong Ying, and Daniel Sjöberg. "Performance analysis of millimeter-wave phased array antennas in cellular handsets." IEEE Antennas and Wireless Propagation Letters 15, 504-507,2015.
[15] Naqvi, Aqeel Hussain, and Sungjoon Lim. "Review of recent phased arrays for millimeter-wave wireless communication." Sensors 18, no. 10,3194, 2018.
[16] Nickel, Ulrich. Fundamentals of signal processing for phased array radar. Fgan-fhr research inst for high frequency physics and radar techniques wachtberg (germany), 2006.
[17] Iupikov, O. A., M. V. Ivashina, K. Pontoppidan, P. H. Nielsen, C. Cappellin, Niels Skou, Sten Schmidl Søbjærg, A. Ihle, D. Hartmann, and K. v't Klooster. "An optimal beamforming algorithm for phased-array antennas used in multi-beam spaceborne radiometers." In 2015 9th European Conference on Antennas and Propagation (EuCAP), pp. 1-5. IEEE, 2015.
[18] Saleem, Muhammad, Sidra Naz, and Anila Kauser. "Principle Features of Beamforming and Phase Shift of Phased Array Antennas." In International Conference on Intelligent Technologies and Applications, pp. 130-141, 2018.
[19] N. Narukawa, T. Fukushima, K. Honda, and K. Ogawa, "64 × 64 MIMO Antenna Arranged in a Daisy Chain Array Structure at 50 Gbps Capacity 2 . 64 × 64 MIMO Beam Steering Array Arranged in a Dasiy Chain Array Structure," 2019 URSI Int. Symp. Electromagn. Theory, pp. 1–4, 2019.
[20] Ruggeri, Eugenio, Apostolos Tsakyridis, Christos Vagionas, George Kalfas, Ruud M. Oldenbeuving, Paul WL van Dijk, Chris GH Roeloffzern, Yigal Leiba, Nikos Pleros, and Amalia Miliou. "Flexible 360° 5G mmWave small Cell Coverage through WDM 4× 1 Gb/s Fiber Wireless Fronthaul and a Si3N4 OADM-Assisted Massive MIMO Phased Array Antenna." In 2020 Optical Fiber Communications Conference and Exhibition (OFC),IEEE, pp. 1-3. 2020.
[21] Moon, Cheon-Bong, Jin-Woo Jeong, Kyu-Hyun Nam, Zhou Xu, and Jun-Seok Park. "Design and Analysis of a Thinned Phased Array Antenna for 5G Wireless Applications." International Journal of Antennas and Propagation 2021.
[22] Chieh, Jia-Chi Samuel, Everly Yeo, Raif Farkouh, Alejandro Castro, Maxwell Kerber, Randall B. Olsen, Emmanuel J. Merulla, and Satish Kumar Sharma. "Development of flat panel active phased array antennas using 5G silicon RFICs at Ku-and Ka-bands." IEEE Access pp.192669-192681,2020.
[23] Lee, Hojoo, Sungpeel Kim, and Jaehoon Choi. "A 28 GHz 5G phased array antenna with air-hole slots for beam width enhancement." Applied Sciences vol.9, no. 20, 4204, 8 , 2020.
[24] W. Theunissen, V. Jain, and G. Menon, "Development of a Receive Phased Array Antenna for High Altitude Plat- form Stations using Integrated Beamformer Modules," 2018 IEEE/MTT-S Int. Microw. Symp. - IMS, pp. 779–782, 2018.
[25] Gao, Huaqiang, Weimin Wang, Wei Fan, Fengchun Zhang, Zhengpeng Wang, Yongle Wu, Yuanan Liu, and Gert Frølund Pedersen. "Design and experimental validation of

automated millimeter-wave phased array antenna-in-package (AiP) experimental platform." IEEE Transactions on Instrumentation and Measurement vol.70, pp.1-11., 2020.

[26] Singhal, Naina, and SM Rezaul Hasan. "Review and comparison of different limited scan phased array antenna architectures." International Journal of Circuit Theory and Applications vol.49, no. 10,pp.3111-3130, 2021.

[27] Mirmozafari, Mirhamed, Shahrokh Saeedi, Guifu Zhang, and Yahya Rahmat-Samii. "A crossed dipole phased array antenna architecture with enhanced polarization and isolation characteristics." IEEE Transactions on Antennas and Propagation vol.68, no. 6, pp.4469-4478,2020.

[28] Kim, Ilkyu, and Jeong-Hae Lee. "Theoretical calculation of power densities in the near-field region of phased array antenna." Microwave and Optical Technology Letters 63, no. 1, 367-371,2021.

[29] Hanson, Jordan C. "Broadband rf phased array design with meep: Comparisons to array theory in two and three dimensions." Electronics vol.10, no. 4 415,2021.

[30] Z. Wang, C. Pang, Y. Li, and X. Wang, “Phased Array Antenna,” IEEE Antennas Wirel. Propag. Lett.,no.c,p.1,2019.